

5. We thank F. Matsubara, N. Suzuki, and M. Ohshima for permission to reproduce one of their figures before publication, and Y. Suzuki, P. Beauvillain, J. Miltat, A. Thiaville, N. Hosoito, K. Mibu, S. Isoda, and H.

Miyajima for valuable discussions. Supported by a Grant-in-Aid for Creative Basic Research from Monbusho, by the New Energy and Industrial Technology Development Organization (NEDO), and by a Japan

Society for the Promotion of Science (JSPS) postdoctoral fellowship (R.H.).

8 March 2000; accepted 14 June 2000

High-Gain Harmonic-Generation Free-Electron Laser

L.-H. Yu,^{1*} M. Babzien,¹ I. Ben-Zvi,¹ L. F. DiMauro,¹ A. Doyuran,¹ W. Graves,¹ E. Johnson,¹ S. Krinsky,¹ R. Malone,¹ I. Pogorelsky,¹ J. Skaritka,¹ G. Rakowsky,¹ L. Solomon,¹ X. J. Wang,¹ M. Woodle,¹ V. Yakimenko,¹ S. G. Biedron,² J. N. Galayda,² E. Gluskin,² J. Jagger,² V. Sajaev,² I. Vasserman²

A high-gain harmonic-generation free-electron laser is demonstrated. Our approach uses a laser-seeded free-electron laser to produce amplified, longitudinally coherent, Fourier transform-limited output at a harmonic of the seed laser. A seed carbon dioxide laser at a wavelength of 10.6 micrometers produced saturated, amplified free-electron laser output at the second-harmonic wavelength, 5.3 micrometers. The experiment verifies the theoretical foundation for the technique and prepares the way for the application of this technique in the vacuum ultraviolet region of the spectrum, with the ultimate goal of extending the approach to provide an intense, highly coherent source of hard x-rays.

The invention of the laser provided a revolutionary source of coherent light that created many new fields of scientific research. Modern laser technology provides versatile performance throughout much of the electromagnetic spectrum. Optical resonators exist in the infrared, visible, and ultraviolet regions of the spectrum, whereas nonlinear optics is used to extend coverage toward shorter wavelengths (<200 nm). However, the small nonlinear susceptibilities available at short wavelengths result in inefficient photon up-conversion. Thus, an important objective in optical physics is the development of coherent intense sources at short wavelengths. Work to accomplish this is proceeding in several directions. In particular, there have been advances in high-harmonic (1) and x-ray (2, 3) sources generated from intense laser-atom interactions and advances in the development of plasma lasers (4). However, in the hard x-ray regime (1 Å), the free-electron laser (FEL) emerges as a promising source that is capable of producing unprecedented intensities (5). Like synchrotron radiation sources, FELs are based on accelerator technology. FELs represent an advance over synchrotron radiation, because in an FEL the radiation process benefits from multiparticle coherence, whereas synchrotron radiation is emitted incoherently by independently radiating electrons. Consequently, FELs offer the possibility of combining the intensity and coher-

ence of a laser with the broad spectral coverage of a synchrotron.

Several configurations of an FEL source are illustrated in Fig. 1. The most widespread configuration involves the use of a high- Q optical cavity (Q , quality factor) (6) and is very effective in wavelength regimes where appropriate mirrors are available. As in the case of lasers, the use of an optical resonator can provide a high degree of spatial and temporal coherence. Conversely, the strategy for developing a hard x-ray FEL (7) uses a high-gain, single-pass amplifier scheme to circumvent the lack of high-quality resonator mirrors at short wavelengths. A straightforward approach to single-pass amplification is referred to as self-amplified spontaneous emission (SASE) (8–21). In SASE, the spontaneous radiation emitted by quivering electrons near the beginning of a long undulator magnet is subsequently amplified as it copropagates with the electron beam through the magnetic structure. This process is capable of producing output with high peak power and excellent spatial mode, but a limitation imposed by the random noise buildup is poor temporal coherence, i.e., coherence time that is much less than pulse duration.

In this report, we describe an alternative single-pass FEL approach, high-gain harmonic generation (HGHG) (22–24), capable of providing the intensity and spatial coherence of SASE but with excellent temporal coherence. Our work was stimulated by earlier theoretical (25, 26) and experimental (27, 28) studies of harmonic generation. In the HGHG FEL, a small energy modulation is imposed on the electron beam by interaction with a seed laser in a short undulator (the

modulator). The energy modulation is converted to a coherent spatial density modulation as the electron beam traverses a dispersion magnet (a three-dipole chicane). A second undulator (the radiator), tuned to a higher harmonic of the seed frequency ω , causes the microbunched electron beam to emit coherent radiation at the harmonic frequency $n\omega$, followed by exponential amplification until saturation is achieved. The HGHG output radiation has a single phase determined by the seed laser, and its spectral bandwidth is Fourier transform limited.

A major advantage of the HGHG FEL is that the output properties at the harmonic wavelength are a map of the characteristics of the high-quality fundamental seed laser. This results in a high degree of stability and control of the central wavelength, bandwidth, energy, and duration of the output pulse. As the duration of the HGHG radiation reflects the seed pulse characteristics, the output radiation pulse can be made shorter than the electron bunch length by simply using an appropriate duration seed laser pulse synchronized to the electron beam. In fact, high-peak-power output pulses of a few femtoseconds are possible with chirped pulse amplification (CPA) (29). On the other hand, a short SASE pulse requires an equally short electron bunch, which is presently beyond the state of the art below a few hundred femtoseconds. More problematic is that the temporal profile of the SASE output varies because of the uncontrollable statistical fluctuations of the shot noise that provides the starting signal, and the SASE output is not Fourier transform limited but is a superposition of many wave trains with phases determined by individual electrons.

At the Accelerator Test Facility at Brookhaven National Laboratory, we performed a proof-of-principle experiment to test the theoretical foundations of the HGHG process. By seeding an FEL at a wavelength of 10.6 μm provided by a CO₂ laser, we observed saturated amplified output at the second-harmonic wavelength, 5.3 μm (30). The HGHG pulse energy was measured to be $\sim 10^7$ times as large as the spontaneous radiation and $\sim 10^6$ times as large as the SASE signal, which, in the case of the HGHG experiment, provides a background noise.

A schematic of the HGHG apparatus with typical operational parameters is illustrated in Fig. 2 (31). The source of the required high-brightness electron beam is the s-band photocathode radio frequency (RF) electron gun (32). The 40-MeV electron beam employed in this experiment is characterized by a current of 120 A [0.8 nC in 6 ps full width at half maximum (FWHM)] with a normalized emit-

¹Brookhaven National Laboratory, Upton, NY 11973, USA. ²Advanced Photon Source, Argonne National Laboratory, Argonne, IL 60439, USA.

*To whom correspondence should be addressed. E-mail: lhyu@bnl.gov

tance of 5 mm-mrad and a global energy spread of 0.6%. Operating the radiator in SASE mode (no CO₂ laser), the 5.3- μm SASE power was measured to be 13 times the spontaneous output (power observed in absence of gain), in good agreement with theoretical simulations. The SASE measurement was performed with a 2% bandwidth, a 5.3- μm band-pass filter, and a calibrated InSb detector.

Seeding the modulator with 200-ps, 10.6- μm CO₂ laser light with a peak power of 0.5 MW, we observed intense HGHG output at the second-harmonic wavelength of 5.3 μm . Increasing the attenuation of the filter preceding the InSb detector, we determined that the HGHG signal was 3×10^6 times as large as the SASE signal produced in the same length of radiator (1.98 m). The HGHG pulse energy was independently measured with a Joule meter. The maximum output observed was 65 μJ .

The spectral distribution of the FEL output was characterized with two methods. A scanning (multipulse) measurement provided sufficient sensitivity for characterizing both the SASE and HGHG output. A single-shot imaging technique provided a more precise measure of the HGHG spectrum, but it lacked the sensitivity for a

SASE measurement. Figure 3A shows the multipulse measurement. The SASE output is multiplied by a factor of 10^6 for comparison to the HGHG spectrum. Each SASE point is an average of 10 shots, whereas the HGHG data are single shots normalized to the total HGHG pulse energy. The FWHM HGHG bandwidth is ~ 20 nm, whereas the SASE bandwidth is six times as large. The HGHG single-shot spectrum was recorded by placing a thermal imaging camera at the exit plane of the spectrometer. The measured spectrum is shown in Fig. 3B and has a FWHM bandwidth of 15 nm.

Theory provides an important predictive tool for the push toward hard x-rays. Simulation of the current experiment was carried out with a modified version of the three-dimensional axisymmetric code (23). In this model, the radiation process is simulated with the Maxwell equations coupled to the classical equations describing the electron motion. A Monte Carlo method provides a random distribution of the initial conditions. Our calculation ignores slippage effects. This is a reasonable approximation for our parameters because the electron bunch length (6 ps) is much longer than the slippage distance (1 ps). With the measured electron beam longitudinal profile (current versus time), the model predicts a FWHM of the HGHG pulse of 3.5 ps. The radiation pulse is narrowed relative to the electron pulse (6 ps FWHM) because the gain is largest in regions of high current. For a Fourier transform-limited (Gaussian) pulse of time duration $(\Delta t)_{\text{FWHM}}$, the ratio of the bandwidth to the central wavelength λ is

$$\left(\frac{\Delta\lambda}{\lambda}\right)_{\text{FWHM}} = \frac{2 \ln 2}{\pi} \frac{\lambda}{c(\Delta t)_{\text{FWHM}}}$$

where c represents the speed of light. Using this approximation and taking $(\Delta t)_{\text{FWHM}} = 3.5$ ps and $\lambda = 5.3$ μm , one finds $(\Delta\lambda/\lambda)_{\text{FWHM}} = 0.22\%$. However, the resolution of the spectrometer measurement is 0.1%. Thus, theory predicts an observable bandwidth of

$\sqrt{0.22^2 + 0.1^2} = 0.24\%$, in good agreement with the measured value of $(\Delta\lambda/\lambda)_{\text{FWHM}} = 15$ nm/5.3 $\mu\text{m} = 0.28\%$.

After the radiator, the electron beam is sent through an energy spectrometer. The image of the transverse horizontal profile reveals the energy distribution, which is observed to exhibit a double peak. The largest peak is shifted to lower energy by 1%, i.e., close to the magnitude of the Pierce parameter. The double peak as observed is characteristic of the electron energy distribution at saturation. Also, the output radiation power is insensitive to input laser power and charge fluctuation. This provides strong evidence that the system is in saturation.

Our simulation predicts a saturated HGHG peak power output of 35 MW. Assuming an HGHG pulse duration of 3.5 ps, we estimate a pulse energy of 120 μJ , in reasonable agreement with the measured pulse energy of 65 μJ . In the future, a direct measurement of the HGHG pulse length will be performed with a second-harmonic intensity autocorrelator.

The success of the current HGHG investigation provides a promising roadmap toward shorter wavelengths. The next step is a facility [deep ultraviolet-FEL (DUV-FEL)] (33) capable of vacuum ultraviolet operation. In contrast to the present study, the DUV-FEL will use a higher energy linear accelerator (linac) (210 MeV) coupled with a 10-m-long undulator (NISUS) (34). A magnetic bunch compressor is installed after 70 MeV of linac, and the source of electrons is an s-band photocathode RF gun. A tunable titanium-sapphire laser drives the photocathode at 266 nm (third harmonic of Ti³⁺:Al₂O₃) and will also provide the seed for the HGHG FEL. Initial operation in the visible will investigate control of the temporal profile of the output radiation and implementation of CPA for ultrashort pulse operation. Following the initial work in the visible, we plan to operate in the vacuum ultraviolet and use the output radiation in a series of proof-of-principle science experiments.

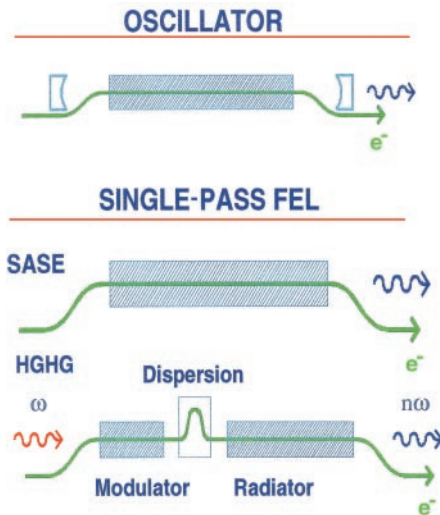


Fig. 1. FEL configurations. **(top)** Oscillator. The use of an optical resonator offers many benefits in wavelength regimes where suitable mirrors exist. **(middle)** SASE. SASE corresponds to the use of a single-pass FEL in which the starting signal is the radiation emitted by the electrons at the beginning of the undulator magnet. **(bottom)** HGHG. HGHG is a single-pass FEL in which a laser seed induces an energy modulation in the electron beam in the first undulator. This energy modulation is converted into a coherent spatial density modulation in the dispersion magnet, and radiation at the n th harmonic of the seed laser wavelength is generated and amplified to saturation in the second undulator.

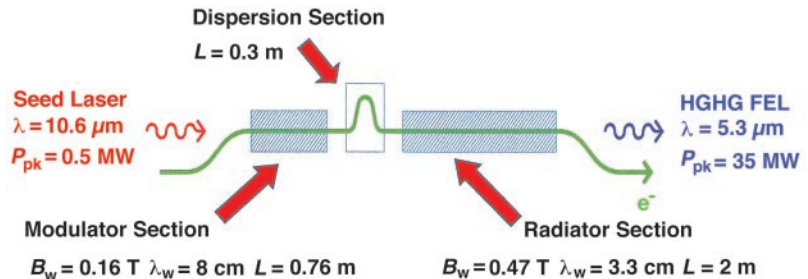


Fig. 2. Configuration for the HGHG FEL experiment as carried out at the Accelerator Test Facility at Brookhaven National Laboratory. The 40-MeV electron beam had a current of 120 A (0.8 nC in 6 ps) with a normalized emittance of 5 mm-mrad. L , length; λ , wavelength; P_{pk} , peak power; B_w , peak undulator magnetic field; λ_w , undulator period.

This investigation has experimentally demonstrated the fundamental principles of HGHG FEL operation. The HGHG approach offers an alternative and attractive FEL scheme that combines the benefits of the coherence properties of a laser with the short-wavelength capabilities of an accelerator-based light source. A future x-ray HGHG FEL could use the best advances in short-wavelength tabletop lasers as seeds for amplifying and pushing toward shorter wavelengths. We are examining a number of different options for hard x-ray operation. For example, the cascading of several HGHG stages (35) can provide a route for x-ray generation using current near-ultraviolet seed laser performance. In this approach, the output of one HGHG stage provides the input seed to the next. Each stage is composed of a modulator, dispersion section, and radiator. Within a single stage, the frequency is multiplied by a factor of 3 to 5. For each stage, the coherent

radiation produced by the prebunched beam in the radiator at the harmonic of the seed is many orders of magnitude higher in intensity than the SASE generated. In a specific example (35), after cascading five HGHG stages, the frequency of the output is a factor of $5 \times 5 \times 5 \times 4 \times 3 = 1500$ times the frequency of the input seed to the first stage. Dispersion sections are placed between stages to shift the radiation to fresh portions (36) of the electron bunch to avoid the loss of gain due to the energy spread induced in the previous stage.

et al., there is exponential growth in the modulator but not in the radiator, whereas in our approach, there is exponential growth in the radiator but not in the modulator. In the approach by Bonifacio et al., the exponential growth process in the modulator is allowed to proceed close to saturation, producing so much energy spread in the electron beam that, although there is coherent harmonic emission in the radiator, there is not exponential amplification of the harmonic radiation. To overcome this critical shortcoming, we introduced a dispersion section between the modulator and radiator (which Bonifacio et al. do not have). As a result, in HGHG, the interaction of the electron beam with the laser seed needs only to take place over a short distance. The small energy modulation produced in the modulator is converted into spatial bunching in the dispersion section. Then, in the radiator, the bunched electron beam first radiates coherently at a harmonic of the seed as in the scheme of Bonifacio et al., but then is exponentially amplified because we were careful to produce only a small energy spread. The exponential amplification that takes place after the coherent harmonic emission is absolutely critical, and it distinguishes our approach from others. In fact, this amplification of the harmonic radiation is the property that we think will allow HGHG to surpass the intensity achievable at short wavelengths from high harmonic generation in nonlinear media using high-power ultrashort-pulse lasers. In HGHG, the amplified harmonic output power is an order of magnitude larger than the power of the longer wavelength input seed. This unique property opens the possibility of cascading several stages of HGHG to achieve very short wavelengths.

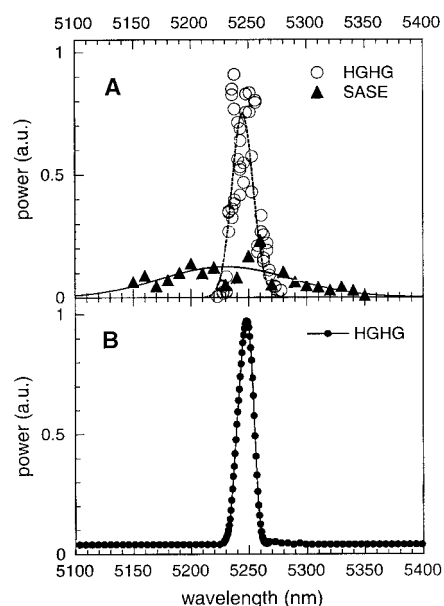


Fig. 3. Output spectrum. (A) Scanning multi-pulse measurements of the output power spectrum for HGHG and SASE, on the experimental apparatus illustrated in Fig. 2. The graph plots power (in arbitrary units) against wavelength (in nanometers). The HGHG FEL bandwidth is one-sixth the SASE bandwidth. The SASE data are multiplied by a factor of 10^6 to bring them onto the same scale as the HGHG results. The SASE amplifier could achieve the same power level as the HGHG FEL if the radiator undulator was made three times longer, but the SASE bandwidth would still be larger than that of the HGHG device. The solid line is a fit to the SASE spectral line, and the dashed line is a fit to the HGHG spectral line. (B) The HGHG single-shot spectrum as recorded by a thermal imaging camera placed at the exit plane of the spectrometer. The graph plots power (in arbitrary units) against wavelength (in nanometers). FWHM bandwidth is 15 nm.

References and Notes

1. P. Salieres, A. L'Huilier, P. Antoine, M. Lewenstein, *Adv. At. Mol. Opt. Phys.* **41**, 83 (1998).
2. J. C. Kieffer et al., *Phys. Fluids B* **5**, 2676 (1993).
3. A. Rousse et al., *Phys. Rev. E* **50**, 2200 (1994).
4. D. C. Eder et al., in *X-ray Lasers 1996*, vol. 151 of *Institute of Physics Conference Series*, S. Svanberg and C. G. Wahlstrom, Eds. (Institute of Physics, Bristol, UK, 1996), pp. 136–142.
5. S. Leone, "Report of the BESAC Panel on Novel Coherent Light Sources" (U.S. Department of Energy, Washington, DC, 1999).
6. Recent work at the Thomas Jefferson National Accelerator Facility (Newport News, VA) using an FEL oscillator operating in the infrared achieved an output average power of >1 KW [G. R. Neil et al., *Phys. Rev. Lett.* **84**, 662 (2000)].
7. LCLS Design Study Group, "Linac Coherent Light Source (LCLS) Design Study Report," Report No. SLAC-R-521 (Stanford Linear Accelerator Center, Stanford, CA, 1998) (available at <http://www.slac.stanford.edu/pubs/slacreports/slac-r-521.html>).
8. Y. S. Debenev, A. M. Kondratenko, E. L. Saldin, *Nucl. Instrum. Methods Phys. Res. A* **193**, 415 (1982).
9. R. Bonifacio, C. Pellegrini, L. Narducci, *Opt. Commun.* **50**, 373 (1984).
10. J. M. Wang and L. H. Yu, *Nucl. Instrum. Methods Phys. Res. A* **250**, 484 (1986).
11. K. J. Kim, *Nucl. Instrum. Methods Phys. Res. A* **250**, 396 (1986).
12. ———, *Phys. Rev. Lett.* **57**, 1871 (1986).
13. S. Krinsky and L. H. Yu, *Phys. Rev. A* **35**, 3406 (1987).
14. L. H. Yu, S. Krinsky, R. L. Gluckstern, *Phys. Rev. Lett.* **64**, 3011 (1990).
15. ———, J. B. J. van Zeijts, *Phys. Rev. A* **45**, 1163 (1992).
16. R. Bonifacio, L. De Salvo, P. Pierini, N. Piovella, C. Pellegrini, *Phys. Rev. Lett.* **73**, 70 (1994).
17. L. H. Yu, *Phys. Rev. E* **58**, 4991 (1998).
18. S. Krinsky, *Phys. Rev. E* **59**, 1171 (1999).
19. B. W. J. McNeil, G. R. M. Robb, D. A. Jaroszynski, *Opt. Commun.* **165**, 65 (1999).
20. SASE gain of 10^5 at 12 μm was reported by M. J. Hogan et al. [*Phys. Rev. Lett.* **81**, 4867 (1998)].
21. SASE gain at 530 nm was recently observed at the Low-Energy Undulator Test Line Facility at the Advanced Photon Source (APS)/Argonne National Laboratory (Argonne, IL) (S. V. Milton et al., in preparation) and at 110 nm at the TeV-Energy Superconducting Linear Accelerator Test Facility/Deutsche Elektronen-Synchrotron (Hamburg, Germany) (J. Rossbach et al., in preparation).
22. I. Ben-Zvi, L. F. Di Mauro, S. Krinsky, M. White, L. H. Yu, *Nucl. Instrum. Methods Phys. Res. A* **304**, 151 (1991).
23. L. H. Yu, *Phys. Rev. A* **44**, 5178 (1991).
24. I. Ben-Zvi et al., *Nucl. Instrum. Methods Phys. Res. A* **318**, 208 (1992).
25. I. Boscolo and V. Stagno, *Nucl. Instrum. Methods Phys. Res.* **198**, 483 (1982).
26. R. Bonifacio, L. de Salvo Souza, P. Pierini, E. T. Scharlemann, *Nucl. Instrum. Methods Phys. Res. A* **296**, 787 (1990). Our development of HGHG (9) was strongly influenced by this earlier work of Bonifacio et al. However, HGHG differs in a critically important way from the earlier work. In the scheme of Bonifacio
27. R. Prazeres et al., *Nucl. Instrum. Methods Phys. Res. A* **304**, 72 (1991).
28. D. A. Jaroszynski, R. Prazeres, F. Glotin, O. Marcouille, J. M. Ortega, *Nucl. Instrum. Methods Phys. Res. A* **375**, 456 (1996). In this work, the authors demonstrated the influence of harmonic prebunching in an FEL oscillator with low gain, using two undulators with harmonically related periods.
29. L. H. Yu, E. Johnson, D. Li, D. Umstadter, *Phys. Rev. E* **49**, 4480 (1994).
30. Preliminary results of the HGHG experiment were presented by L. H. Yu et al. [paper presented at the 21st Free Electron Laser Conference, Hamburg, Germany, 23 to 26 August, 1999].
31. The modulator is a magnet originally built as a prototype for the National Synchrotron Light Source soft x-ray undulator at beamline X1, and the radiator is the prototype for the APS undulator A, which was at one time installed and tested in the Cornell Electron Storage Ring at Cornell University (Ithaca, NY). Both of these magnets were remeasured and shimmed to provide the required field quality for the HGHG experiment. A new electromagnet was built to serve as the dispersion section.
32. X. Qiu, K. Batchelor, I. Ben-Zvi, X. J. Wang, *Phys. Rev. Lett.* **76**, 3723 (1996).
33. I. Ben-Zvi et al., in *Proceedings of the 18th International Free Electron Laser Conference, Rome, August 26–31, 1996*, G. Datoli and A. Renieri, Eds. (Elsevier, Amsterdam, 1997), pp. II-10, II-11.
34. The 10-m-long NISUS undulator was originally built by STI Optronics for use in a visible FEL at Boeing.
35. Recent theoretical work on generating hard x-rays by cascading HGHG stages of successively shorter wavelength has been carried out by L. H. Yu and J. H. Wu [in *Proceedings of the ICFA 17th Advanced Beam Dynamics Workshop on Future Light Sources*, C. E. Eyberger, Ed. (Argonne National Laboratory, Argonne, IL, 1999) (available at <http://www.aps.anl.gov/conferences/FLSworkshop/proceedings/papers/wg1-o1.pdf>)].
36. L. H. Yu and I. Ben-Zvi, *Nucl. Instrum. Methods Phys. Res. A* **393**, 96 (1997).
37. This work was supported by the U.S. Department of Energy, Office of Basic Energy Sciences, under contract numbers DE-AC02-98CH10886 and W-31-109-ENG-38 and by Office of Naval Research grant number N00014-97-1-0845.

23 February 2000; accepted 19 June 2000